Electronic supplementary information

Nonsolvent induced reconfigurable bonding configurations of ligands in nanoparticles purification

Jun Zhang[1,#], Falin Tian[2,#], Min Zhang[3], Tiefeng Li[4], Xueqian Kong[1,*] Yunlong Zhou[2,3,*], and Nicholas A. Kotov[5]

1. Center for Chemistry of High-Performance & Novel Materials, Department of Chemistry, Zhejiang University, Hangzhou, Zhejiang 310027, China.

2. Engineering Research Center of Clinical Functional Materials and Diagnosis & Treatment Devices of Zhejiang Province, Wenzhou Institute, University of Chinese Academy of Sciences, Wenzhou, Zhejiang 325000, China.

3. School of Biomedical Engineering, School of Ophthalmology and Optometry and Eye Hospital, Wenzhou Medical University, Wenzhou, Zhejiang 325011, China.

4. Institute of Applied Mechanics, Zhejiang University, Hangzhou, Zhejiang 310027, China.

5. Department of Chemical Engineering, and Biointerfaces Institute, University of Michigan, Ann Arbor, Michigan 48109, United States.

Corresponding Authors

*kxq@zju.edu.cn (X. K.)

*zhouyl@wibe.ac.cn (Y. Z.)

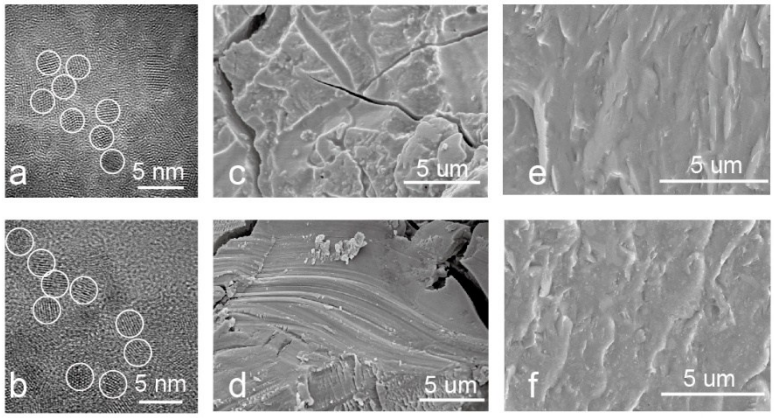

Fig. S1. HRTEM images of (a) 2.7 nm NPs and (b) 3.2 nm NPs. The SEM images of (c) gel-1:1-2.7, (d) gel-1:1-3.2, (e) gel-1:3-2.7 and (f) gel-1:3-3.2.

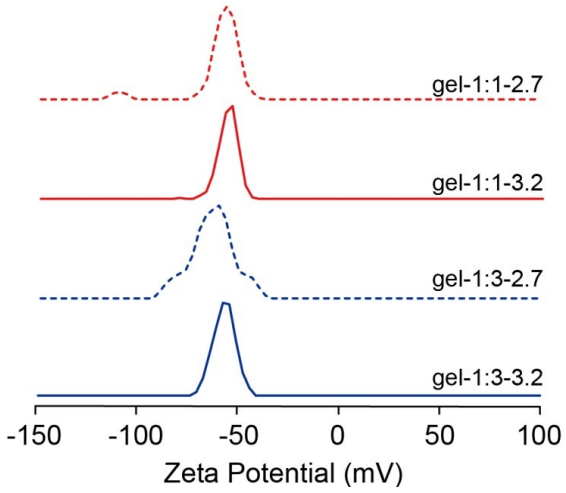

Fig. S2. Zeta potential measurement of the diluted hydrogels solution, gel-1:1-2.7 (red dotted line), gel-1:1-3.2 (red line), gel-1:3-2.7 (blue dotted line), gel-1:3-3.2 (blue line).

After removing the supernatant, the viscous liquid of CdTe NPs was dissolved in 1 mL deionized water for Zeta potential tests. As indicated in Fig. S2, the zeta potential of NPs, corresponding to the three hydrogels, are -55.5 mV for gel-1:1-2.7, -62.9 mV for gel-1:3-2.7, -55.3 mV for gel-1:1-3.2 and -55.7 mV for gel-1:3-3.2, respectively. Zeta potential with highly negative charged NPs indicates good stability in aqueous solution. The NP purified by 1:3 IPA was more stable than that by 1:1 volume ratio, which can be explained as more ligands benefit the NP stability.

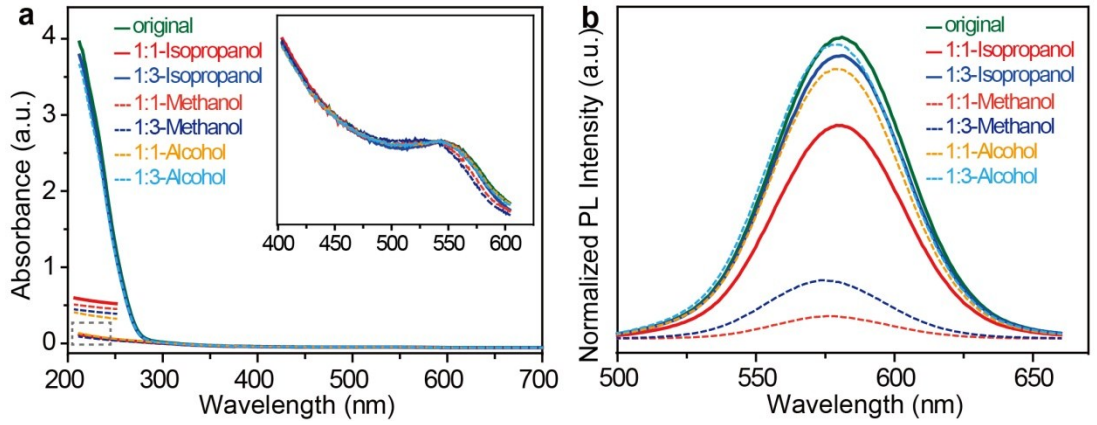

Fig. S3. (a) UV-Vis spectra and (b) Normalized PL spectra ($\lambda_{ex} = 450\ nm$) of the CdTe NP dispersions precipitated by different alcohols.

The effects of nonsolvent, that is, methanol, ethanol, and IPA on CdTe NPs coated with MPA were studied in detail. All of the NP can be precipitated by these nonsolvent, demonstrating by the same first excitonic absorption peak in UV-Vis spectra of the purified NP solution with that of the original solution. In the UV spectra, the absorption below 300 nm was mainly contributed by the Cd-MPA complexes. For the comparisons of nonsolvent effect on purification efficiency, the absorption of the Cd-MPA complexes in v_{NP}:$v_{nonsolvent}$=1:1 was significantly reduced, while there was no obvious change in v_{NP}:$v_{nonsolvent}$=1:3 (Fig. S3a). After purified by methanol, ethanol, and isopropanol with 1:1 and 1:3, the normalized PL intensity of the NPs weakened to different degrees. For the same nonsolvent (e.g. IPA), UV-Vis absorption and PL intensity of 1:1 is lower than that of the 1:3, owing to the decreased quantity of Cd-MPA complexes.

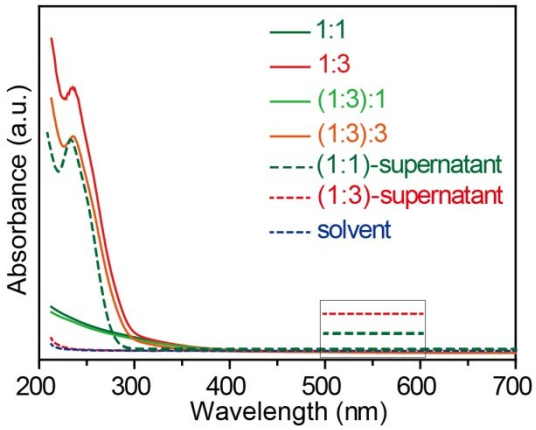

Fig. S4. UV-Vis spectra of the CdTe NP dispersions with different purification methods using isopropanol.

Once the NP precipitating from v_{NP}:v_{IPA}=1:3 solutions, its supernatant showed that there was no obvious UV-Vis signal between 200 nm to 300 nm. The NP precipitates were re-dispersed in deionized water to get the same concentration of the original solution, which was purified again by IPA with a volume ratio of 1:1 and 1:3. It was found that (1:3):3 retained many Cd-MPA complexes compared with (1:3):1. The results showed that the removal of Cd-MPA complexes was independent of the purification times and related to the IPA dosage. Furthermore, UV-Vis results of the 1:1 and 1:3 supernatant showed no first exciton absorption peak about 550 nm, indicating that the nanoparticles were completely precipitated.

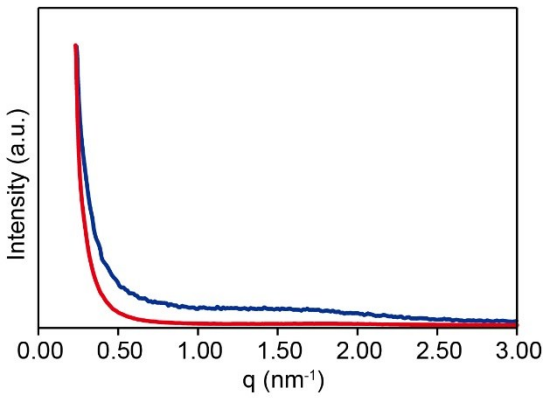

Fig. S5. The SAXS measurements of the gel-1:1-3.2 (red line) and gel-1:3-3.2 (blue line).

The SAXS results show zero characteristic peaks for gel-1:1-3.2 and gel-1:3-3.2, which means nanoparticles in hydrogels have similarly random structures. For gel-1:3-3.2, the signal between 1.0 – 2.0 nm^{-1} shows that there are some differences in electronic distribution between organic ligands and inorganic core. In other words, the inorganic cores of gel-1:1-3.2 are relatively close to each other compared with that of the gel-1:3-3.2, which can be explained as fewer ligands reduce the distance between NPs.

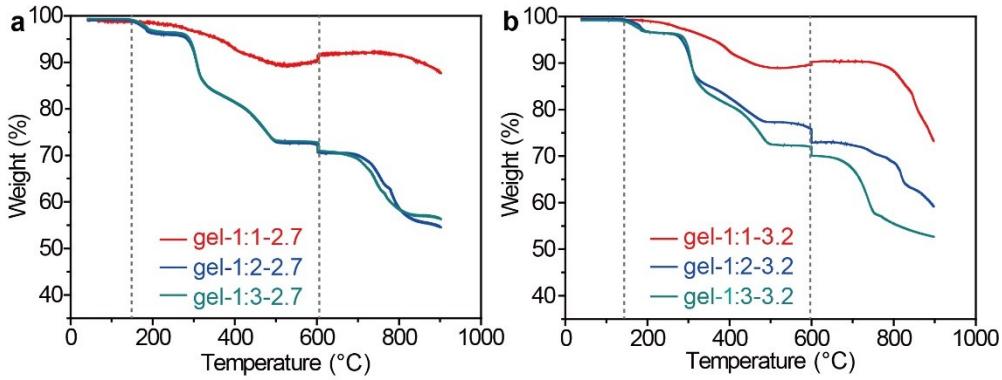

Fig. S6. Weight loss from TGA measurement for CdTe NP gels with the core size of (a) 2.7 nm and (b) 3.2 nm. The rate of temperature increase was 5 °C/min and experiments were performed under N_2 atmosphere.

As shown in Fig. S6, the gels began to lose water under 150 °C and weak ligands began to decompose at ～300 °C. At 600 °C (most organic ligands decomposed), weight loss% is 9.8%, 26.2%, 26.8%, 10.8%, 22.4%, and 26.8% for gel-1:1-2.7, gel-1:2-2.7, gel-1:3-2.7, gel-1:1-3.2, gel-1:2-3.2 and gel-1:3-3.2, respectively. The TGA data under 600 °C showed that the losses of organic ligands in v_{NP}:v_{IPA}=1:2 and v_{NP}:v_{IPA}=1:3 were similar, manifesting two or three-volume IPA had the same purification efficiency for CdTe NP gels. This work mainly focuses on the purification difference caused by one and three-volume IPA. At the temperature higher than 600 ℃, there are also some residual strong ligand maintaining burning.[1] Hence, the organic matter mass should be equal to the sum of the weak ligand and the strong ligand. Together with elemental analysis, therefore, the TGA data were not only used to qualitatively distinguish purification efficiency of the particle purified by different volume IPA, but also was further used to calculate extra Cd cations.

Tab. S1. Elemental analysis Carbon and hydrogen content of Cd-MPA complexes purified with and without IPA.

Sample	Weight (mg)	C%	H%	Organic%	Inorganic%
Cd-MPA	2.0014	11.7	2.5	34.6	65.4
	1.9818	11.4	2.6	33.8	66.2
Cd-MPA-1:1	2.0274	17.4	2.9	51.3	48.7
	1.9955	16.6	3.0	49.2	50.8
Cd-MPA-1:3	1.8299	18.1	3.8	53.6	46.4
	1.7337	16.4	3.5	48.4	51.6

To evaluate whether the IPA could also partly affect the Cd-MPA complexes, we prepared NP precursor (Cd-MPA complexes) following the first step of preparation of NPs (method, first step). Compared with crude Cd-MPA complexes, Cd-MPA-1:1 and Cd-MPA-1:3 have reduced a large amount of inorganic components. Elemental analysis showed the IPA can effectively remove unreacted inorganic ions.

Tab. S2. Elemental analysis Carbon and hydrogen content of gel-1:1-3.2 and gel-1:3-3.2

Sample	Weight (mg)	W_C%	W_H%	$W_{Organic}$%	$W_{Inorganic}$%
gel-1:1-3.2	1.9542	8.1	1.7	23.8	76.2
	1.9033	8.0	1.8	23.7	76.3
gel-1:3-3.2	2.0003	18.6	3.3	54.9	45.1
	1.9446	18.2	3.8	53.9	46.1

According to the elemental analysis results in Table S2, the ligand proportions of gel-1:1-3.2 and gel-1:3-3.2 are ~24% and ~55%, which show that the ratio of IPA controls the purification efficiency of NP solutions.

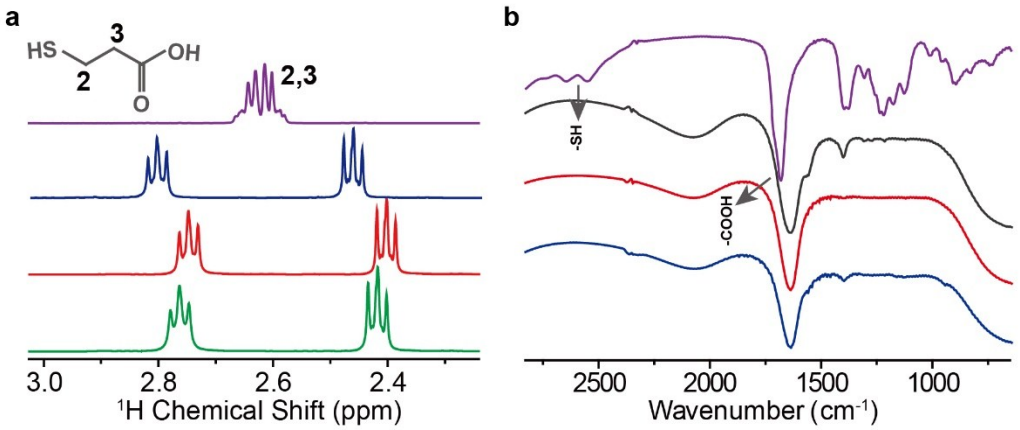

Fig. S7. (a) The ^{1}H NMR spectrum of MPA (purple line), Cd-MPA (blue line), Cd-MPA-1:1 (red line) and Cd-MPA-1:3 (green line) in deuterium oxide. (b) The FTIR of MPA (purple line), Cd-MPA (grey line), gel-1:1-3.2 (red line) and gel-1:3-3.2 (green line).

Fig. S7a shows the 1D ^{1}H spectra of MPA and Cd-MPA. The hydrogen resonances at carbons 2 and 3 (free MPA) overlap together, and the two signals separate when the functional groups (carboxyl or sulfhydryl) bind to cadmium ion (Cd-MPA complexes). In the ^{1}H NMR spectra, the ^{1}H chemical shifts of Cd-MPA complexes purified by one-volume and three-volume IPA decrease by 0.5 - 0.6 ppm in comparison with that of crude Cd-MPA complexes because some of the inorganic ions were removed by IPA; this is in agreement with the elemental analysis results of Cd-MPA complexes (Table S1). By removing these inorganic ions, the electron density around the protons increases and the chemical shift decreases.

gel-1:1-3.2 and gel-1:3-3.2 in Fig. S7b show same results that the stretching of sulfhydryl group (–SH) at about 2600 cm^{-1} disappears and the stretching (1400 – 1475 cm^{-1}) of the carboxy group (COOH) at about 1650 cm^{-1} retains strong absorption, suggesting that the sulfhydryl group coordinates the particle surface in both 1:1 and 1:3 particle dispersions.

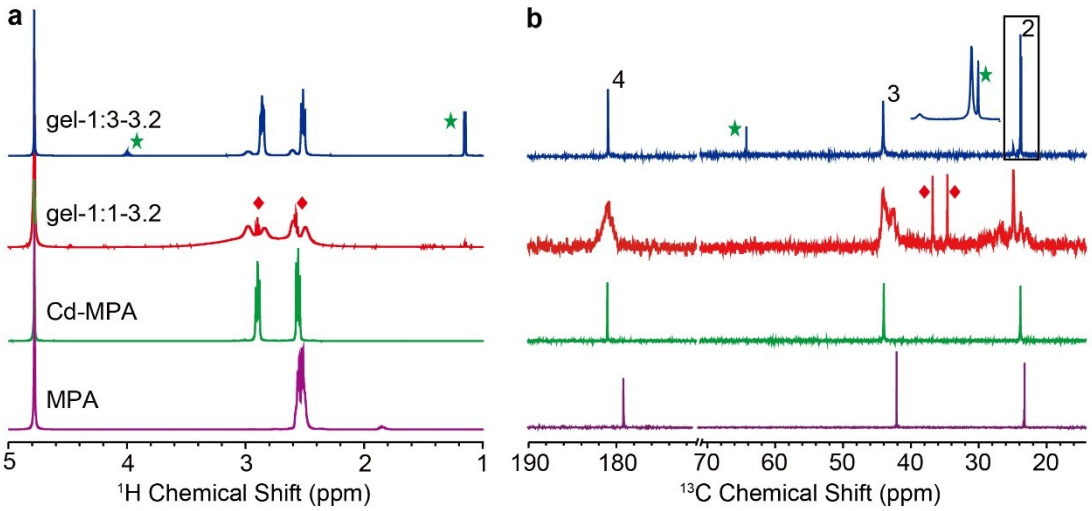

Fig. S8. (a) ^{1}H NMR spectra and (b) ^{13}C NMR spectra of MPA (purple line), Cd-MPA complexes (green line), gel-1:1-3.2 (red line) and gel-1:3-3.2 (blue line). The peaks marked with the green stars belong to IPA, and the peaks marked with red rhombus belong to DTDPA.

As shown in the ^{1}H NMR spectra (Fig. S8), gel-1:3-3.2 contains a small amount of IPA positioned at ~ 1.15 ppm with dual peaks (J coupling constant = 6.2 Hz) and ~ 4.00 ppm with small multiplets (J value = 6.1 Hz). Here, in the gel-1:1-3.2 dispersion, the unknown component at 2.47 ppm and 2.82 ppm shows the small triplets with J coupling constant 7.0 Hz, matching well with the dithiodipropionic acid (DTDPA) purchased from the reagent company. The ^{13}C signals of the IPA and DTDPA can also be observed in the ^{13}C NMR spectra, and the correlation between ^{1}H and ^{13}C signals was built by HSQC in Fig. S9.

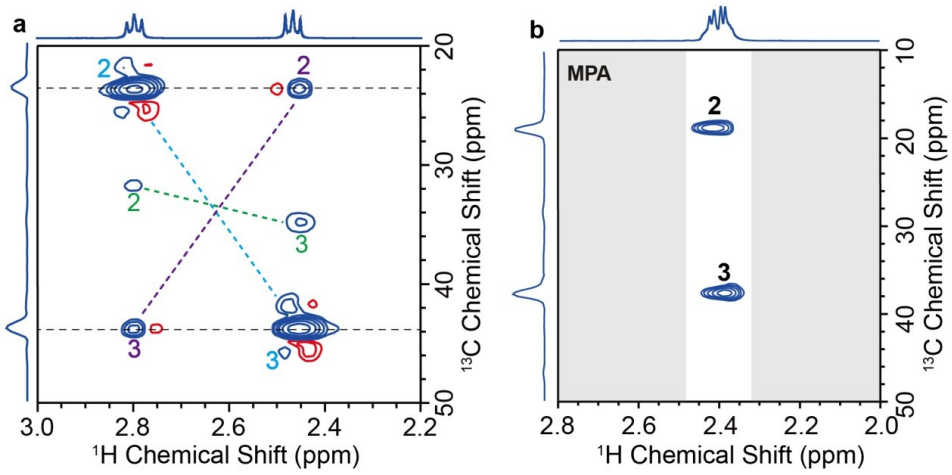

Fig. S9. (a) ^{1}H-^{13}C HSQC spectrum of Cd-MPA complexes in deuterium oxide. The same color marks (the dotted lines and numbers) belong to the same component. (b) ^{1}H-^{13}C HSQC spectra of MPA. The alpha- and beta-methylene carbon atoms of sulfhydryl correspond to number 2 and 3, respectively.

The HSQC shows that there are three components in Cd-MPA complexes. The proton resonances overlap in the 1D ^{1}H spectrum, which indicates there are two types of cadmium salts and one kind of byproduct (DTDPA) — 83% (MPA)S-Cd complexes (blue dotted line), 12% (MPA)COO-Cd complexes (purple dotted line), 5% DTDPA (green dotted line).

We used the HSQC of MPA to verify the reliability of the quantitative method in Fig. S9b. Since the signal overlay of the row slice overlaps, we extracted the column slice. The slices are extracted in the white area and superposed together, then a new 1D spectrum is formed. The integral ratio of the signal at 39 pm and 19 ppm has a 10% deviation, which can be tolerated to differentiate Cd-MPA forms.

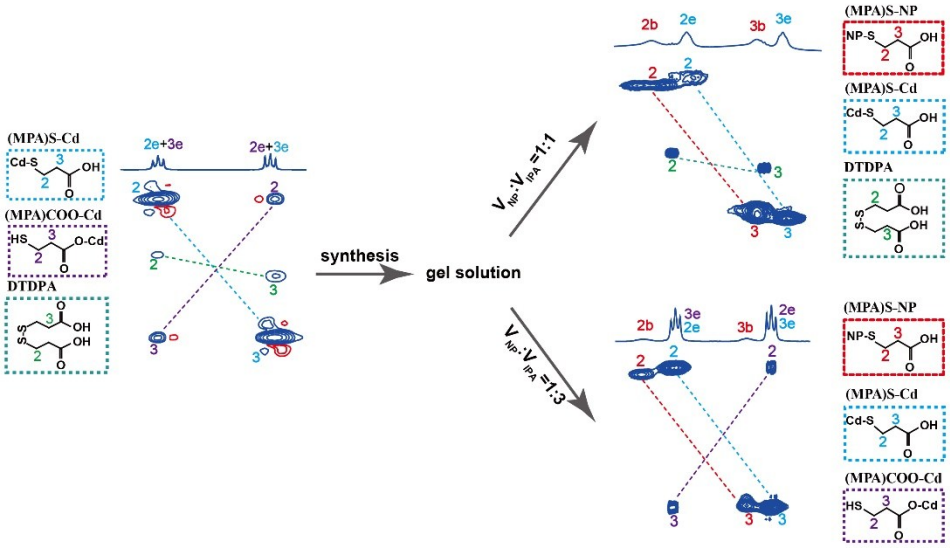

Fig. S10. Scheme for the correlation of ligand molecular structures (H and C) and the different potential situations (free/bound) to the HSQC spectra.

Table S3. The compositions in gel-1:1-3.2 and gel-1:3-3.2 samples by analysis of ^{1}H-^{13}C HSQC spectrum. The relative proportion is determined by integrating resonances of ^{1}H NMR spectra or column slices extracted from HSQC.

Sample	(MPA)S-NP	(MPA)S-Cd	(MPA)COO-Cd	DTDPA	IPA
gel-1:1-3.2	63.0%	37.0%	-	2.0%	-
gel-1:3-3.2	14.0%	65.0%	16.0%	-	5.0%

We also obtained elemental analysis for gel-1:1-3.2 and gel-1:3-3.2 (Table S2) and found organic mass ratios of 23.8 % and 54.4 %, respectively. Combining each component and its molar proportion (Table S3) retained in the NP solution, the inorganic ($(MPA)S\text{–}NP_{\text{ion.}}\%$) and organic ($(MPA)S\text{–}NP_{\text{org.}}\%$) mass ratios of the NP can be obtained according to the following formula.

In gel-1:1-3.2

$$(\mathrm{MPA})\mathrm{S}-\mathrm{NP}_{org}\,\% = (\mathrm{NP}-1:1)_{org}\,\% - [(\mathrm{MPA})\mathrm{S}-\mathrm{Cd}]_{org}\,\% - \mathrm{DTDPA}\,\% \quad (1)$$

$$(\mathrm{MPA})\mathrm{S}-\mathrm{NP}_{ino}\,\% = (\mathrm{NP}-1:1)_{ino}\,\% - [(\mathrm{MPA})\mathrm{S}-\mathrm{Cd}]_{ino}\,\% \quad (2)$$

In gel-1:3-3.2

$$(\mathrm{MPA})\mathrm{S}-\mathrm{NP}_{org}\,\% = (\mathrm{NP}-1:3)_{org}\,\% - [(\mathrm{MPA})\mathrm{S}-\mathrm{Cd}]_{org}\,\% - [(\mathrm{MPA})\mathrm{COO}-\mathrm{Cd}]_{org}\,\% - \mathrm{IPA}\,\% \quad (3)$$

$$(\mathrm{MPA})\mathrm{S}-\mathrm{NP}_{ino}\,\% = (\mathrm{NP}-1:3)_{ino}\,\% - [(\mathrm{MPA})\mathrm{S}-\mathrm{Cd}]_{ino}\,\% - [(\mathrm{MPA})\mathrm{COO}-\mathrm{Cd}]_{ino}\,\% \quad (4)$$

Therefore, the mass ratios of bound ligands and the inorganic core of gel-1:1-3.2 are 15.0 % and 71.5 %, respectively, and those of gel-1:3-3.2 are 7.4 % and 22.8 %, respectively. The 3.2 nm CdTe NP was structured with spherical approximation, containing 375 Cd atoms and 284 Te atoms, and the molar mass of the core is $78392.2\ g/mol$.

Table S4. The weight ratios of the bound ligand and inorganic core in CdTe NP gels.

Weight ratio	gel-1:1-3.2	gel-1:3-3.2
W_{ligand}%	17.3%	24.5%
W_{core}%	82.7%	75.5%

According to the elemental analysis results (Table S2) and NMR data from Table S3, the mass ratios of bound ligands and the inorganic core can be obtained and are presented in Table S4. The average number of bound ligands per nanoparticle (n_{Ligand}) can be calculated by the following formula.

$$W_{ligand}\% = \frac{n_{ligand} \times M_{ligand}}{n_{ligand} \times M_{ligand} + M_{core}} \quad (5)$$

This equation can be also rewritten as

$$n_{ligand} = \frac{W_{ligand}\% \times M_{core}}{M_{ligand} \times (1 - W_{ligand}\%)} \quad (6)$$

Here, $M_{ligands} = 104.4\ g/mol$, which is the molar mass of MPA. $M_{core} = 78392.2\ g/mol$. The $W_{ligand}\%$ is the relative mass ratio of bound ligands relative to the mass of the nanoparticle. Therefore, the number of bound ligands is 158 for gel-1:1-3.2 and 241 for gel-1:3-3.2. In addition, the average number of adsorbed ligands (i.e. (MPA)S-Cd complexes) per nanoparticle can be determined based on the proportional relation between adsorbed ligands and bound ligands. In gel-1:1-3.2, the adsorbed ligands are 0.6 times that of the bound ligands equaling to ~ 95, and in gel-1:3-3.2, the adsorbed ligands are 4.6 times that of the bound ligand equaling to ~ 1120.

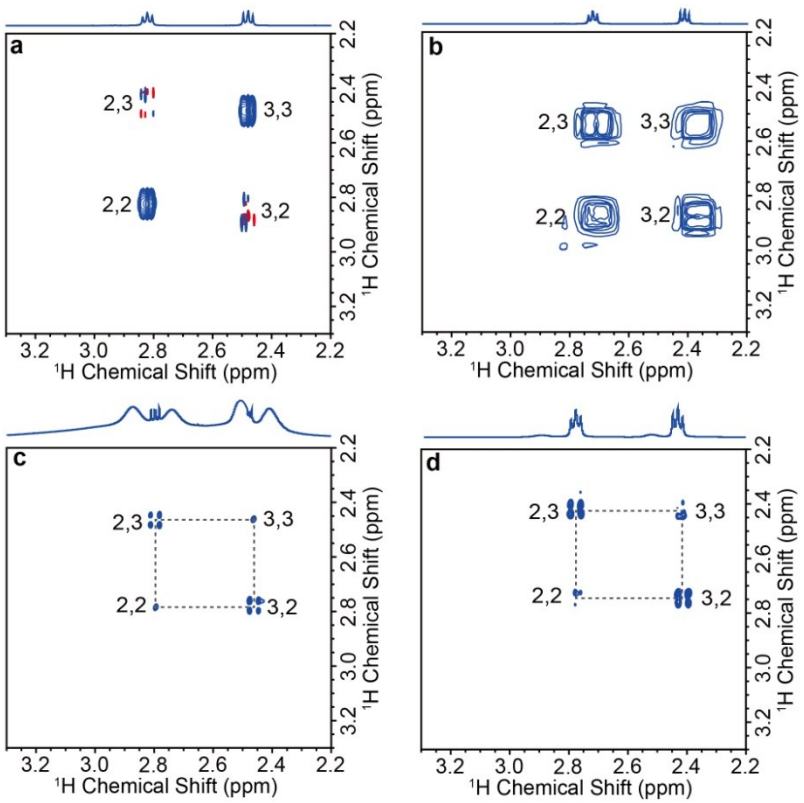

Fig. S11. (a) NOESY of Cd-MPA complexes. COSY of (b) Cd-MPA complexes, (c) gel-1:1-3.2, and (d) gel-1:3-3.2.

The NOESY of Cd-MPA complexes shows negative correlation peaks (red contours) to the peaks on the diagonal, which are characteristic of small molecules. In COSY, Cd-MPA complexes have obvious cross peaks generated by J coupling. When the ligands are in contact with the NP surface, the increased T2 relaxation diminished their COSY signals. In Fig. S10c & d, only the free DTDPA, and part of free ligands generate the cross peaks of J coupling.

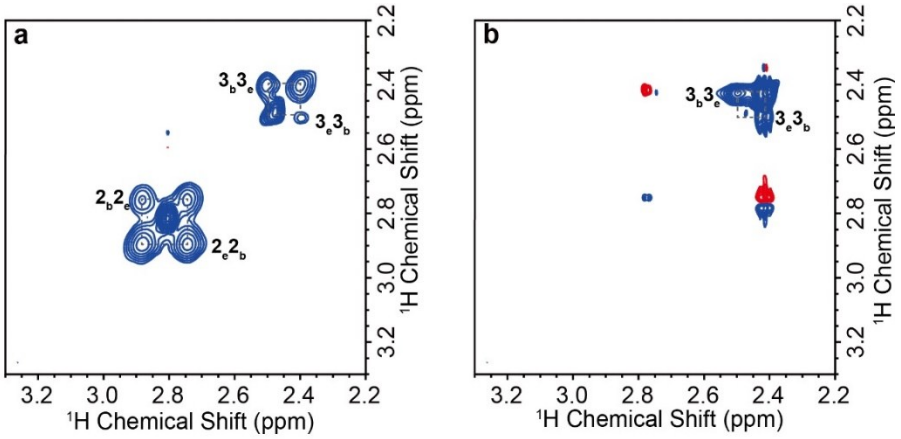

Fig. S12. ROESY spectrum of (a) gel-1:1-3.2 and (b) gel-1:3-3.2 in deuterium oxide. The carbon atoms of sulfhydryl alpha-methylene and beta-methylene are marked with number 2 and 3, respectively. The bound ligands and free ligands are represented by the letters b and e, respectively.

The ROESY experiment (Fig. S11a & 11b) show that the 2_b2_e, 2_e2_b, 3_b3_e and 3_e3_b are the chemical exchange cross peaks, keeping the same sign with the diagonal peaks, which means that they originate mainly from the chemical exchange of free ligands between the bound ligands and not from cross-relaxation.[2]

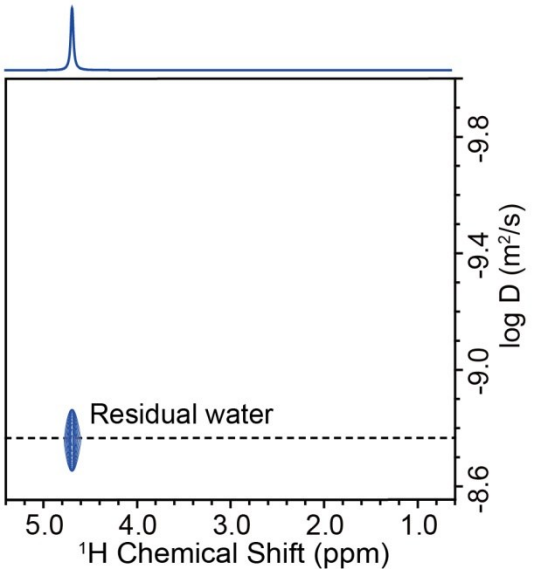

Fig. S13. DOSY spectra of deuterium oxide solution. The diffusion coefficient of residual water is about 1.7×10^{-9} m^2/s.

Calculation the binding energy between MPA ligand and CdTe NPs. To study the interaction between MPA molecules and CdTe NPs, two types of coordinating positions, that are, two facets cleaved along the (100) and (111) directions to model the surface of the NPs (Fig. S12). Briefly, the bulk crystal structure of CdTe was optimized firstly, then the two facets were cleaved and optimized further. After that, an optimized MPA anion was added with an idealized starting position to the two optimized facets respectively, and further optimizations were performed, in which the CdTe nanoclusters were kept fixed. Finally, when the optimizations finished, the binding energies were calculated as in Eq. 7

$$E_{bind} = -\left(E_{total} - E_{facet} - E_{MPA} + 1/2E_{H_2}\right) \quad (7)$$

Where E_{bind} is the binding energy of the MPA, E_{total} is the energy of the CdTe facet cluster with the MPA anion adsorbed, E_{facet} is the energy of the CdTe facet cluster, E_{MPA} is the energy of the free MPA ligand, and E_{H_2} is the energy of the H_2. Each of the optimized energy in Eq. 7 was listed in Table S5.

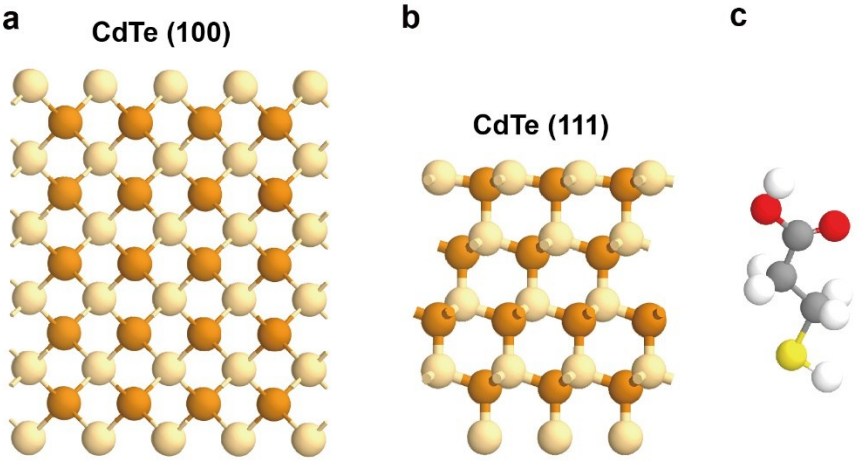

Fig. S14. (a) and (b) The optimized structure of the CdTe NP; (c) MPA molecule.

Table S5. The energy for calculating the binding energies for MPA anions on CdTe NP facet.

System	E_{total}(eV)	E_{facet}(eV)	E_{MPA}(eV)	E_{H_2}(eV)	E_{bind}(eV)
MPA/CdTe(100)-I	-243.12	-178.28	-66.92	-6.76	**1.30**
MPA/CdTe(100)-II	-242.74	-178.28	-66.92	-6.76	**0.92**
MPA/CdTe(111)	-226.58	-162.34	-66.92	-6.76	**0.70**

To determinate the physical interaction between MPA bonded on the CdTe and free MPA-Cd complexes, an optimized MPA-Cd complex was placed on an idealized starting position to interact with an MPA ligand bound to two optimized facets, respectively (Fig. S13), and further optimizations were performed. The CdTe nanoclusters were kept fixed, while MPA and MPA-Cd could move freely. The energies between CdTe nanoclusters and free MPA-Cd complex were calculated as in Eq. 8

$$E_{interaction} = -\left(E_{total} - E_{bind} - E_{MPA-Cd}\right) \quad (8)$$

Where $E_{interaction}$ is the interaction energy of the CdTe and free MPA-Cd complex, E_{total} is the system energy of the CdTe facet cluster with the MPA anion adsorbed and an MPA-Cd complex, E_{bind} is the energy of the CdTe facet cluster with the MPA anion adsorbed, E_{MPA-Cd} is the energy of the free MPA-Cd complex. Each of the optimized energy in Eq. 8 was listed in Table S6.

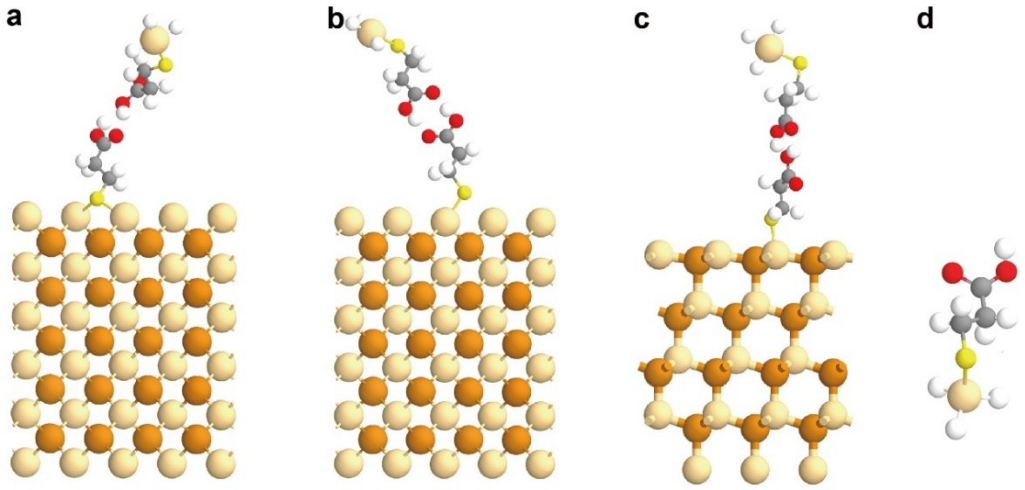

Fig. S15. (a) – (c) The optimized structures of bounded MPA-CdTe interacting with free MPA-Cd complex; (d) The optimized MPA-Cd complex.

Table S6. The interaction energies for CdTe NPs and free MPA-Cd complexes.

system	E_{total}(eV)	E_{bind}(eV)	E_{MPA-Cd}(eV)	$E_{interaction}(eV)$
MPA-Cd/CdTe(100)-I	-314.66	- 243.12	- 71.16	**0.38**
MPA-Cd/CdTe(100)-II	- 314.13	- 242.74	- 71.16	**0.23**
MPA-Cd/CdTe(111)	- 297.92	- 226.58	- 71.16	**0.18**

The binding structure of MPA coated on the CdTe surface. To study the binding structure of MPA molecule on CdTe NPs, two different kinds of binding positions, i.e., the face and the edge of the NPs, were considered like our previous works.[3] Briefly, two parts of the clusters were constructed as the base for calculations (Fig. S14), one of which contained 20 cadmium (Cd) atoms and 16 tellurium (Te) atoms to represent the edge of the NPs, and the other with 17 Cd atoms and 10 Te atoms in a cluster represent the face of the NPs. In the simulation, both the Te and Cd ions on the NP surface were capped by H atoms, and the MPA connected on the face or edge of the NPs by S-Cd group. The positions of the Cd and Te atoms of the CdTe cluster were frozen during the simulation. For the Cd-MPA complex, it was presented by one MPA molecule connected to a Cd atom by Cd-S group, and it could move freely during the simulation (Fig. S14). All the simulations performed using the software package Spartan (WavefuNPtion INP., Irvine, CA). After building up the atomic model of one NP cluster, its geometry was first optimized by using the Merck molecular force field (MMFF). Then the MPA molecule coated on the cluster through S-Cd group and the cluster-MPA structure was optimized to its lowest energy structure. Finally, using the equilibrium geometry, we calculated the binding energy between the MPA and the cluster using the semiempirical parameter model 3 (PM3) method, which typically gives good estimates of the interaction of inorganic structures with transition metals.[4,5]

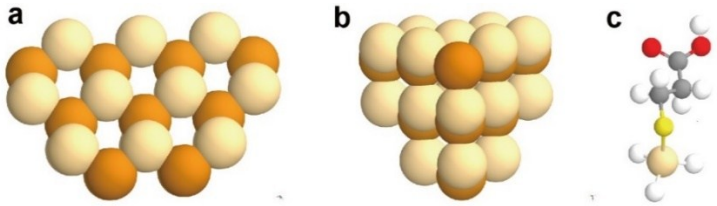

Fig. S16. The optimized calculation structures: (a) The edge of the NPs, (b) The facet of the NPs, (c) The MPA molecule.

References:

1. Anush, S. M.; Vishalakshi, B. Modified Chitosan Gel Incorporated with Magnetic Nanoparticle for Removal of Cu(II) and Cr(VI) from Aqueous Solution. *Int. J Biol Macromol.* **2019,** *133*, 1051-1062.

2. Hens, Z.; Martins, J. C. A Solution NMR Toolbox for Characterizing the Surface Chemistry of Colloidal Nanocrystals. *Chem. Mater.* **2013**, *25(8)*, 1211-1221.

3. Zhou, Y.; Damasceno, P. F.; Somashekar, B. S.; Engel, M.; Tian, F.; Zhu, J.; Huang, R.; Johnson, K.; McIntyre, C.; Sun, K.; Yang, M.; Green, P. F. Ramamoorthy, A.; Glotzer, S. C.; Kotov, N. A. Unusual Multiscale Mechanics of Biomimetic Nanoparticle Hydrogels. *Nature Commun.* **2018**. *9*, 181.

4. Zhou, Y.; Yang, M.; Sun, K.; Tang, Z.; Kotov, N. A. Similar Topological Origin of Chiral Centers in Organic and Nanoscale Inorganic Structures: Effect of Stabilizer Chirality on Optical Isomerism and Growth of CdTe Nanocrystals. *J. Am. Chem. Soc.* **2010**, *132(17)*, 6006-6013.

5. Wang, Y. C.; Ludwigson, M.; Lakes, R. S. Deformation of Extreme Viscoelastic Metals and Composites *Mater. Sci. Eng. A.* **2004**, *370(1-2)*, 41-49.